Crystal Morphology Control of LTL-Type Zeolite Crystals

Olivier Larlus and Valentin P. Valtchev*

Laboratoire de Matériaux Minéraux, UMR-7016 CNRS, ENSCMu, UHA, 3 rue Alfred Werner, 68093 Mulhouse Cedex, France

Received January 22, 2004. Revised Manuscript Received June 15, 2004

The effects of the chemical composition of the starting gel, aging time, and crystallization temperature on the crystal size and morphology of zeolite L were studied. The chemical variables were the water content, concentration of potassium hydroxide, substitution of potassium by sodium, introduction of small amounts of barium, and the Si/Al ratio of the initial gel. The changes in the crystal morphology were evaluated by the aspect ratio of the prismatic ((100) and (1−10)) and pinacoidal (001) faces. The water content in the system was found to have the most pronounced effect on this ratio, providing crystals with a prismatic/pinacoidal face ratio between 0.5 and 3. Among the other chemical parameters, the alkalinity of the system had a pronounced effect on the nucleation and thus on the ultimate crystal size. The effects of potassium/sodium substitution and the introduction of barium in the starting gel on the zeolite L morphology were negligible. The interdependence of the chemical variables, crystallization temperature, and aging time and their impact on the crystal size and morphology is discussed. The crystal size and morphology of zeolite L were also influenced by the variation of the aging time and crystallization temperature. Thus, long aging of the gel (1−4 weeks) under ambient conditions provided nanosized crystals with narrow particle size distribution, while the increase of crystallization temperatures resulted in the formation of large (4−5 μm) crystals with high prismatic/pinacoidal faces ratios. The study allowed a fine-tuning of the size (from 140 nm to 7 μm) and of the morphology of zeolite L crystals, which varied from long prismatic crystals terminated by a small pinacoid to coin-like crystals with very short prismatic faces and a well-developed pinacoid. The changes in the aspect ratio between prismatic/pinacoidal faces lead to changes in the number of pore openings per total external surface. This number, together with the variation of the length of the prismatic faces, is expected to have an impact on the performance of the material.

Introduction

The performance of bulk materials often depends on the morphology of primary particles, especially in the case of anisotropic crystals, where the required property is characteristic for a particular crystallographic direction. Thus, the close control of crystal morphology is highly desirable for numerous materials including microporous crystals.

Microporous inorganic crystals have found great utilization as catalysts and sorption media due to their large internal surface area, defined channel systems with pore diameters of less than 1 nm, and controlled density of the active sites.[1,2] Because of their unique pore systems, these crystalline materials can impart shape selectivity for both the reactants and the products when processing relatively low molecular weight hydrocarbon feed streams. Besides unique shape selectivity, microporous crystals can display molecular recognition, discrimination, and organization properties with a resolution of less than 1 Å. The performance of microporous zeolite-type crystals is closely related to the type of the channel system, that can be mono-, bi-, or three-dimensional, comprising similar or different sized pores for the latter two types. The crystal morphology for the materials possessing a three-dimensional channel system, for example, FAU- and LTA-type zeolites,[3] is not expected to have a great impact on their properties. In contrast, the performance of materials with mono- or bi-dimensional channel systems might be strongly affected by the morphology of the crystals. Depending on the crystal morphology, the pore openings of a particular channel system can be present at the crystal surface to a different extent. As a consequence, the access to the intracrystalline volume may be facilitated or hindered. The crystal morphology and size define also the diffusion paths via the channels that often have a great impact on the reaction kinetics.

For example, Rajagopalan et al.[4] have investigated the effect of the particle size of zeolite Y in fluid catalytic cracking. This investigation revealed that the smaller crystals exhibit improved activity and selectivity to

* To whom correspondence should be addressed. E-mail: v.valtchev@uha.fr.

(1) Breck, D. *Zeolite Molecular Sieves*; John Wiley and Sons: New York, 1974; p 771.

(2) Szostak, R. *Handbook of Molecular Sieves*; Van Nostrand Reinhold: New York, 1992; p 524.

(3) Baerlocher, Ch.; Meier, W. M.; Olson, D. H. *Atlas of Zeolite Framework Types*, 5th revised ed.; Elsevier: Amsterdam, 2001; p 302.

(4) Rajagopalan, K.; Peters, A. W.; Edwards, G. C. *Appl. Catal.* **1986**, *23*, 69.

10.1021/cm0498741 CCC: $27.50
Published on Web 07/29/2004

intermediate products such as gasoline and light cycle oil. Shiralkar et al.[5] have studied the physicochemical properties of ZSM-5 crystals ranging from 0.3 to 4.0 μm. Their study showed that the increase in the crystal size leads to an inhomogeneous aluminum distribution, which, together with longer diffusion paths, has a strong deteriorative effect on the product yield and selectivity. Several research teams have investigated the effect of the size of zeolite Beta crystals in various catalytic reactions.[6−9] The effect of the crystal size of ZSM-22 on the skeletal isomerization of *n*-butane has also been studied.[10] To the best of our knowledge, the only investigation that tried to correlate crystal morphology with catalytic activity is the work by Bhat et al.[11] devoted to the effect of ZSM-5 crystals with different sizes and morphologies on the toluene ethylation with ethanol. It revealed that the ortho isomer formed on the smaller spherical crystals, while longer crystals of oblong morphology favored the formation of the para isomer. As stated above, the investigation of the effect of zeolite morphology on the physicochemical properties of zeolitic materials has been limited to the impact of crystal size, which is most probably due to the great progress made in this respect during the past decade.[12−17] Therefore, the opportunity for fine-tuning of zeolite properties by varying the crystal morphology is still not fully explored. The reason for this gap in zeolite science seems to be the fact that the morphology of zeolite crystals is far from being controlled, although a number of studies of the effect of the synthesis parameters and the composition of the initial gel on the ultimate crystal size have been performed.[18−22] In addition, various additives, for example, pyrocatechol, triethanolamine, that influence the crystal growth by complex formation with some of the reactants have also been employed.[23−28] It has also been found that zeolite morphology is very sensitive to the reactants, in particular to the silica source selected.[29−32] Thus, although a certain progress in understanding the influence of the different factors controlling the zeolite morphology has been made, the fine-tuning of the morphology of microporous crystals is still to be achieved.

The present study deals with the effect of each component of the initial composition and synthesis parameters on the morphology of zeolite L (LTL-type framework). This zeolite when loaded with Pt exhibits excellent catalytic properties in hexane dehydrogenation,[33,34] and hydrogenation of cinnamaldehyde.[35] Zeolite GL, which is isomorphous with zeolite L, has found industrial application for the aromatization of alkanes.[36] The crystal structure of zeolite L is hexagonal (space group $P6/mmm$) with unit cell constants $a = 18.4$ Å and $c = 7.5$ Å.[37] The linkages of the cancrinite cages (ϵ-cages) by double 6-rings (D6R) lead to the formation of columns in the *c*-direction and thus give rise to 12-membered rings with a free diameter of 7.1 Å.[3] The typical morphology of zeolite L is a combination of two types of hexagonal prisms, (100) and (1−10), and a pinacoidal face (001).[37] The barrel-like crystals of this zeolite are elongated along the *c*-axis, which corresponds to the direction of the monodimensional 12-membered-ring pore system. A shortening of the prismatic faces is expected to lower the diffusion limitations, while an increase of the pinacoidal one would raise the number of pore openings per unit external crystal surface.

The effects of the synthesis parameters on the formation of zeolite L have been studied by several research groups.[38−41] Tsapatsis et al. have used high-resolution transmission and field emission-scanning electron microscopy to study the formation of zeolite L nanocrystals.[38] Special studies have been devoted to the role of alkali earth cations, in particular barium.[42,43] The

(5) Shiralkar, V. P.; Joshi, P. N.; Eapen, M. J.; Rao, B. S. *Zeolites* **1991**, *11*, 511.
(6) Camblor, M. A.; Corma, A.; Iborra, S., Miquel, S.; Primo, J.; Valencia, S. *J. Catal.* **1997**, *172*, 76.
(7) Camblor, M. A.; Corma, A.; Martinez, A.; Martinez-Soria, V.; Valencia, S. *J. Catal.* **1998**, *179*, 537.
(8) Arribas, M. A.; Martinez, A. *Catal. Today* **2001**, *65*, 117.
(9) Landau, M. V.; Vradman, L.; Valtchev, V.; Lezervant, J.; Luibich, E.; Tatianker, M. *Ind. Eng. Chem. Res.* **2003**, *42*, 2773.
(10) Asensi, M. A.; Corma, A.; Martinez, A.; Derewinski, M.; Krysciak, J.; Tamhankar, S. S. *Appl. Catal., A* **1998**, *174*, 163.
(11) Bhat, Y. S.; Das, J.; Rao, K. V.; Halgeri, A. B. *J. Catal.* **1996**, *159*, 368.
(12) Jansen, J. C. *Stud. Surf. Sci. Catal.* **2001**, *137*, 175.
(13) Persson, A. E.; Schoeman, B. J.; Sterte, J.; Otterstedt, J.-E. *Zeolites* **1994**, *14*, 557.
(14) Tsapatsis, M.; Lovallo, M.; Okubo, T.; Davis, M. E. *Mater. Res. Soc. Symp. Proc.* **1995**, *371*, 21.
(15) Camblor, M. A.; Corma, A.; Mifsud, A.; Perez-Pariente, J.; Valencia, S. *Stud. Surf. Sci. Catal.* **1996**, *105A*, 341.
(16) Mintova, S.; Valtchev, V. *Microporous Mesoporous Mater.* **2002**, *55*, 171.
(17) Dong, J.-P.; Zou, J.; Long, Y.-C. *Microporous Mesoporous Mater.* **2003**, *57*, 9.
(18) Bodart, P.; Nagy, J. B.; Derouane, E. G.; Gabelica, Z. *Stud. Surf. Sci. Catal.* **1984**, *18*, 125.
(19) Mostowicz, R.; Berak, J. M. *Stud. Surf. Sci. Catal.* **1985**, *24*, 65.
(20) Camblor, M. A.; Mifsud, A.; Perez-Pariente, J. *Zeolites* **1991**, *11*, 792.
(21) Iwasaki, A.; Sano, T. In *Proc. 12th International Zeolite Conference*; Treacy, M. M. J., Markus, B. K., Bisher, M. E., Higgins, J. B., Eds.; MRS: Baltimore, Warrendale, 1998; Vol. 3, p 1817.
(22) Hamidi, F.; Pamba, M.; Bengueddach, A.; Di Renzo, F.; Fajula, F. *Stud. Surf. Sci. Catal.* **2001**, *135*, 334.
(23) Scott, G.; Thompson, R. W.; Dixon, A. G.; Sacco, A. *Zeolites* **1990**, *10*, 44.
(24) Iwasaki, A.; Sano, T.; Kiyozumi, Y. *Microporous Mesoporous Mater.* **1998**, *25*, 119.
(25) Shao, C.; Qiu, S.; Xiao, F.; Li, X.; Zhai, Q.; Zheng, S.; Zhang, Z. In *Proc. 12th International Zeolite Conference*; Treacy, M. M. J., Markus, B. K., Bisher, M. E., Higgins, J. B., Eds.; MRS: Baltimore, Warrendale, 1998; Vol. 3, p 1701.
(26) Shao, C.; Li, X.; Qiu, S.; Xiao, F.; Terasaki, O. *Microporous Mesoporous Mater.* **2000**, *39*, 117.
(27) Gao, F.; Li, X.; Zhu, X.; Qiu, S.; Wei, B.; Shao, C.; Xiao, F.; Terasaki, O. *Mater. Lett.* **2001**, *48*, 1.
(28) Sano, T.; Wakabayashi, S.; Oumi, Y.; Uozumi, T. *Microporous Mesoporous Mater.* **2001**, *46*, 67.
(29) Sun, Y.; Song, T.; Qiu, S.; Pang, W.; Shen, J.; Jiang, D.; Yue, Y. *Zeolites* **1995**, *15*, 745.
(30) Warzywoda, J.; Dixon, A. G.; Thompson, R. W.; Sacco, A.; Suib, S. L. *Zeolites* **1996**, *16*, 125.
(31) Round, C. I.; Hill, S. J.; Latham, K.; Williams, C. D. *Microporous Mater.* **1997**, *11*, 213.
(32) Mintova, S.; Valtchev, V. *Microporous Mesoporous Mater.* **2002**, *55*, 171.
(33) Grau, J. M.; Daza, L.; Seoane, X. I.; Arcoya, A. *Catal. Lett.* **1998**, *53*, 161.
(34) Jentoft, R. E.; Tsapatsis, M.; Davis, M. E.; Gates, B. C. *J. Catal.* **1998**, *179*, 565.
(35) Li, G.; Li, T.; Xu, Y. *J. Chem. Soc., Chem. Commun.* **1996**, 497.
(36) Han, W.; Kooh, A.; Hicks, R. F. *Catal. Lett.* **1993**, *18*, 219.
(37) Ohsuna, T.; Horikawa, Y.; Hiraga, K.; Terasaki, O. *Chem. Mater.* **1998**, *10*, 688.
(38) Tsapatsis, M.; Lovallo, M.; Okubo, T.; Davis, M. E.; Sadakata, M. *Chem. Mater.* **1995**, *7*, 1734.
(39) Joshi, P. N.; Kotasthane, A. N.; Shiralkar, V. P. *Zeolites* **1990**, *10*, 598.
(40) Wan, Y.; Williams, C. D.; Duke, C. V. A.; Cox, J. J. *Microporous Mesoporous Mater.* **2001**, *47*, 79.
(41) Ko, Y. S.; Chang, S. H.; Ahn, W. S. *Stud. Surf. Sci. Catal.* **2001**, *135*, 189.
(42) Burton, A.; Lobo, R. F. *Microporous Mesoporous Mater.* **1999**, *33*, 97.

detailed investigation of the effect of the gel composition on the size of zeolite L performed by Megelski and Calzaferri[44] provided crystals in the range of 30−3000 nm. These crystals were further used for the preparation of an optical antenna system. The quoted investigations provided precious information of the effect of some of the synthesis variables on the zeolite L crystal size. However, the growth of different faces and their aspect ratios that might have a great effect on the performance of the zeolite were not properly reviewed.

The purpose of the present study was to investigate the effect of the factors that might influence the morphology of the zeolite L crystals so as to achieve a fine control of the crystal habit. Among the goals of the investigation was the increase of the ratio pore openings/crystal surface.

Experimental

Synthesis. The molar composition of the gel used for the synthesis of zeolite L was as follows: $x((1-t)K + tNa)_2O$:yAl_2O_3:$1SiO_2$:zH_2O, where $x = 0.25-0.50$, $y = 0.05-0.2$, $z = 10.0-30.0$, and $t = 0-0.50$. Double distilled water was used for the synthesis and washing of the solid. In a typical preparation, an aluminum powder (99, 97%, Avocado) was dissolved in an alkali hydroxide [(KOH (85%, Fluka); NaOH (96%, Fluka)] solution. Colloidal silica (Ludox HS-40, Dupont) was then added, and the gel was stirred at room temperature for 5 min. The effect of barium was studied in a series of experiments with the following molar composition qBaO:$0.25K_2O$:$0.08Al_2O_3$:$1.0SiO_2$:$15H_2O$, where q is equal to 0.0001, 0.0005, 0.001, and 0.005.

The obtained gels were transferred into Teflon-lined Morey type autoclaves and heated under static conditions at 170 °C for 3 days. In addition, the effects of the aging of the gels at 25 °C (from 1 to 4 weeks), crystallization temperature (from 150 to 200 °C), and synthesis time (from 1 to 3 days) have been investigated.

Characterization. The X-ray diffraction (XRD) patterns of the samples were recorded on a STOE STADI-P diffractometer in Debye−Scherrer geometry equipped with a linear position-sensitive detector (6° in 2θ) and Ge monochromated Cu Kα_1 radiation. The particle size analysis was performed with a dynamic light scattering instrument (DLS, Malvern HPPS-ET). Electron micrographs were taken on a Philips XL30 LaB_6 scanning electron microscope (SEM).

The elemental analyses of the solids were performed by atomic absorption spectroscopy (Varian Techtron AA6) after dissolution in HF. Prior to the addition of HF acid (40%, Carlo Erba) to the purified crystalline product, a given amount of water was added to avoid the evaporation of SiF_4. After the preliminary treatment, each of the elements constituting the crystalline product was analyzed separately.

Results

The reference sample used in this study was prepared from a gel with molar composition $0.25K_2O$:$0.08Al_2O_3$:$1.0SiO_2$:$15H_2O$. According to the XRD measurement, the product was highly crystalline LTL-type material without any traces of other crystalline phases or amorphous material. The SEM inspection showed well-shaped crystals, 2.0−2.5 μm long along the c-direction, with an aspect ratio between the prismatic and pinacoidal faces of about 1.

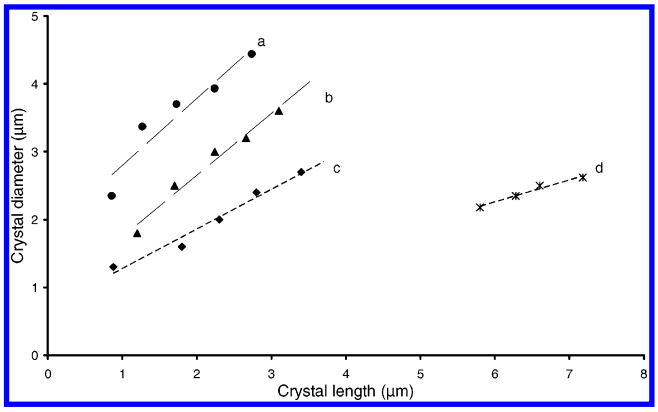

Figure 1. Prismatic/pinacoidal faces ratio for the LTL-type crystals synthesized at different water contents from the gel $0.25K_2O$:$0.08Al_2O_3$:$1.0SiO_2$:zH_2O, where $z = 10$ (a), $z = 15$ (b), $z = 20$ (c), and $z = 25$ (d). Points lying on the straight lines represent different particle classes measured in one batch.

The above composition was systematically changed to study the effect of each of the reactants on the morphology of the crystals.

Effect of the Water Content. The water content (z) in the gel was systematically varied from 10 to 30. These syntheses provided crystals with sizes ranging from 1 to 7 μm, which were not appropriate for investigation by DLS. Thus, the average particle size and particle size distribution of these relatively large particles were obtained via SEM, by measuring about 60 crystals from each sample. Well-faced crystals lying on the prismatic ((100) or (1−10), and (001)) faces allowed collecting representative data for the effect of the water content. The length versus the diameter of the crystals of the different batches is depicted in Figure 1. The experimental points can be linearly interpolated, which suggests that independently of their size, all crystals of a batch have similar length-to-diameter ratios. The linearity of the trends in Figure 1 suggests a fairly linear growth rate during the crystallization stage. Some deviation of the experimental points can be seen in the low-water system (Figure 1a), where the high viscosity of the gel influenced the growth process and as a consequence the ultimate morphology. These measurements showed also gradual changes, that is, a decrease of the length/diameter ratio with an increase of the water content in the system. This effect is evident from the sample synthesized with $z = 25$, where crystals with prismatic/pinacoidal faces ratio of 3 were observed.

These changes in the length-to-diameter ratio had a very pronounced effect on the morphology of the crystals. Thus, at very low water content ($z = 10$), crystals with coin-like morphology and a prismatic/pinacoidal face ratio of about 0.5 were formed (Figure 2a). The calculation was based on the length of the prismatic face without the terrace overgrown on the pinacoidal face (001). As was already stated, the reference composition ($z = 15$) provided almost isometric crystals with a length-to-diameter ratio of about 1 (Figure 2b). The increase of the water content ($z = 20$) resulted in the formation of longer zeolite L crystals with a prismatic/pinacoidal face ratio of about 1.5 (Figure 2c). A further increase of this ratio (ca. 3) was observed when a gel composition with $z = 25$ was employed (Figure 2d). In this case, however, an amorphous halo was detected in the XRD pattern of the material. The composition with

(43) Ferchiche, S.; Warzywoda, J.; Sacco, A. *Stud. Surf. Sci. Catal.* **2001**, *135*, 188.
(44) Megelski, S.; Calzaferri, G. *Adv. Funct. Mater.* **2001**, *11*, 277.

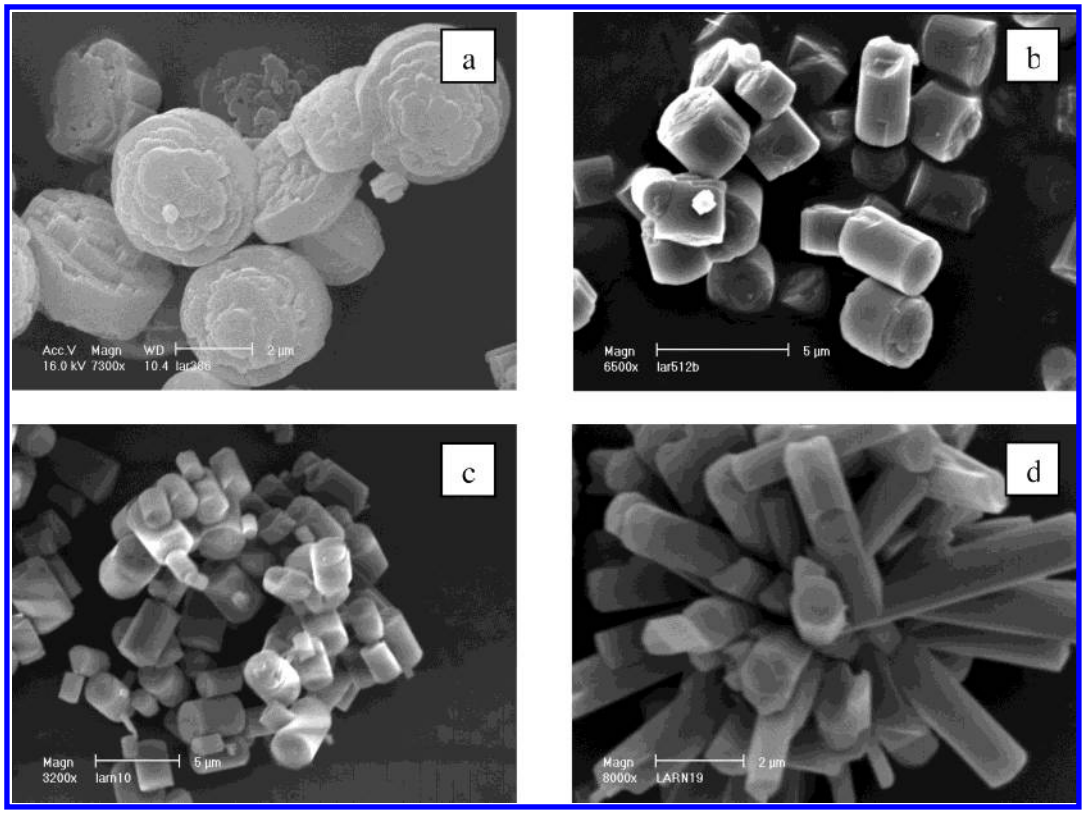

Figure 2. SEM micrographs of the LTL-type crystals synthesized at different water contents from gels of composition $0.25K_2O$: $0.08Al_2O_3$:$1.0SiO_2$:zH_2O, where $z = 10$ (a), $z = 15$ (b), $z = 20$ (c), and $z = 25$ (d).

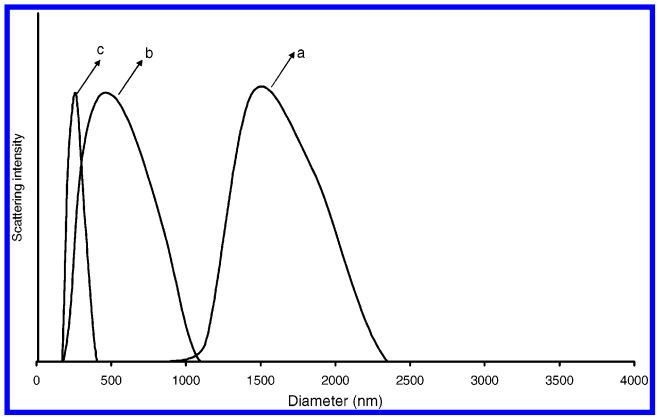

Figure 3. Effect of alkaline hydroxide content on the crystal size of zeolite L synthesized in the system xK_2O:$0.08Al_2O_3$: $1.0SiO_2$:$15H_2O$, where $x = 0.3$ (a), $x = 0.4$ (b), and $x = 0.5$ (c).

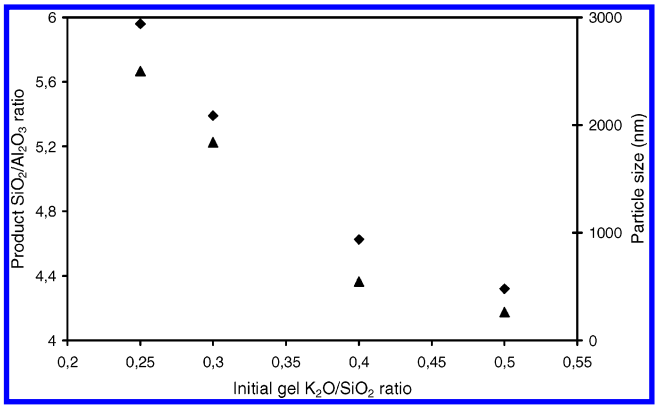

Figure 4. Effect of the potassium hydroxide concentration on the silica-to-alumina ratio (◆) and crystal particle diameter (▲) of the crystalline product.

$z = 30$ did not yield a crystalline material after 3 days of synthesis at 170 °C. It is worth mentioning that the terrace overgrowth on the basic pinacoid observed at $z = 10$ was not very pronounced at $z = 15$ and almost disappeared at higher water contents.

Effect of the Alkalinity. The effect of concentration of potassium hydroxide on the particle size and morphology was studied for the pure potassium system where x varied from 0.25 to 0.50. Two effects of the variation of the KOH content were observed. First, the increase of the alkalinity had a pronounced effect on the crystal size. For example, crystals with an average diameter of 2.5 μm were obtained for $x = 0.25$, while particles of about 150 nm were synthesized with $x = 0.50$. The particle classes obtained by variation of the alkalinity of the system are shown in Figure 3. As can be seen, a gradual decrease of the crystal size is observed with an increase of alkalinity. Second, the variation of the alkalinity controls the particle size distribution, which becomes narrower with the enhancement of the alkali hydroxide (Figure 3). The morphology of the crystals obtained from a gel with $x = 0.25$ is shown in Figure 2b. A gel with $x = 0.35$ provided crystals with shorter prismatic faces and abundant overgrowth on the pinacoidal one. This specific overgrowth of the pinacoidal face imitating bi-pyramidal crystals was also observed for the other compositions with high alkali content ($x = 0.40$ and $x = 0.50$). Besides the effect on crystal morphology, the variation of the alkali concentration had a pronounced effect on the framework composition of the crystals (Figure 4). The decrease of the crystal size, due to the higher KOH concentration in the initial gel, was coupled with a decrease of the Si/Al ratio of zeolite L crystals. Consequently, a larger K^+ content that corresponds to

the framework aluminum was found in the crystals. For instance, the chemical composition of the products synthesized with x equal to 0.3, 0.4, and 0.5 was $K_{9.7}Al_{9.7}Si_{26.3}O_{72}$, $K_{10.9}Al_{10.9}Si_{25.1}O_{72}$, and $K_{11.4}Al_{11.4}Si_{24.6}O_{72}$, respectively.

Effect of the Substitution of K by Na. It is well known that the role of the alkali cations is of primary importance in the synthesis of aluminosilica zeolites.[1] Potassium is the preferred cation as a structure-directing agent in the synthesis of the LTL-type structure.[45] On the other hand, sodium is the cation most widely used in zeolite synthesis, including in the preparation of zeolite L.[40] In the present investigation, up to 50% of KOH was progressively substituted by sodium hydroxide. Highly crystalline solids with LTL-type structure were obtained in the case of substitution degree below 30%. In contrast, the products obtained with higher sodium content were amorphous. Chemical analyses of the crystalline products revealed that the incorporation of sodium in zeolite structure was very limited. For instance, the gel with a 30% substitution of potassium by sodium provided a solid with composition $Na_{0.1}K_{8.9}Al_9Si_{27}O_{72}\cdot 12H_2O$. These data showed that sodium has a structure-breaking rather than a structure-directing effect in the formation of the LTL-type material. Obviously, Na^+ does not match well the zeolite L topology, which is most probably due to the smaller ionic radius (1.02 Å) with respect to the original structure-directing cation (K^+, 1.38 Å).[46] The SEM inspection of the crystalline products did not show any changes in the morphology and crystal size of zeolite L.

Effect of Ba. Barrer[45] has shown that the LTL-type topology can also be synthesized with barium as a structure-directing cation. The structure analysis of the LTL-type material synthesized in the presence of Ba^{2+} has shown that barium and potassium play analogous structure-directing roles due to optimal coordination that both cations have in sites B, C, and D in the LTL-type structure.[43] The similar behavior of Ba^{2+} and K^+ is a function of their close characteristics, in particular the ionic radii, which are 1.36 and 1.38 Å, respectively.[46] The experiments performed in the present study have shown that barium has a very pronounced effect on the size of the zeolite L crystals. Limited amounts of barium added in the initial gel resulted in a substantial decrease of the crystal size (Figure 5). Thus, the addition of 0.005 mol of BaO per 1 mol of SiO_2 provided crystals an order of magnitude smaller than those of the reference sample. Nanocrystals with an average size of about 140 nm were obtained (Figure 5d), whereas the crystals of the reference sample were about 2.5 μm (Figure 2b).

Effect of the SiO_2/Al_2O_3 Ratio. The SiO_2/Al_2O_3 ratio of the initial gel was varied from 5 to 20, which influenced the growth kinetics and purity of the product rather than the morphology of the crystals. At low SiO_2/Al_2O_3 ratio (ca. 5), the system yielded CHA-type zeolite. A pure LTL-type material crystallized in the SiO_2/Al_2O_3 range from 10 to 15. A further increase of the SiO_2/Al_2O_3 ratio resulted in the formation of a mixture of LTL and amorphous material ($SiO_2/Al_2O_3 = 17$), whereas only noncrystalline material was obtained at $SiO_2/Al_2O_3 =$ 20. The LTL-type crystals synthesized in this series of experiments possessed a morphology and crystal size similar to those of the reference sample, independently of the SiO_2/Al_2O_3 ratio of the initial gel.

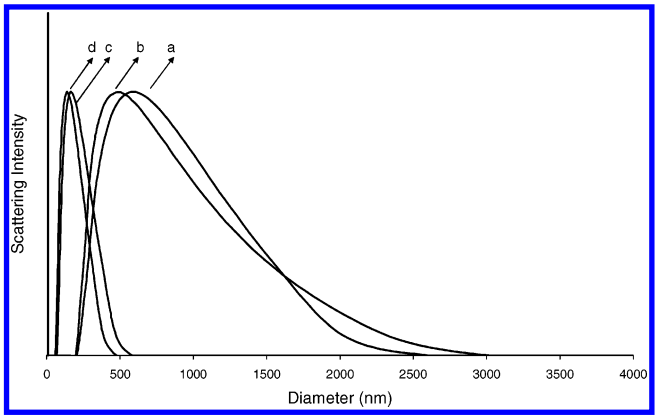

Figure 5. Particle size of zeolite L crystals synthesized by addition of 0.0001 (a), 0.0005 (b), 0.001 (c), and 0.005 mol (d) of BaO per mol of SiO_2.

Effect of Aging. Although zeolite crystallization under laboratory conditions is generally performed at elevated temperatures, it may be strongly influenced by the events taking place in the initial precursor system under ambient conditions. Several groups suggested that structural rearrangements occur during the aging that lead to the formation of zeolite nuclei.[47−50] In the present investigation, the opportunity to nucleate the system under ambient conditions to promote the formation of abundant uniformly distributed nuclei and thus to control the crystal size was studied. The reference gel was aged under ambient conditions from 1 to 4 weeks and was then subjected to hydrothermal treatment. A drastic decrease of the crystal size was observed for all samples (Figure 6). The average crystal size was about 500 nm for all aged samples. This result suggests that the number of nuclei formed in the gels is approximately the same after 1−4 weeks aging. Nevertheless, differences between the samples were observed. The prolongation of the aging time resulted in the crystallization of particles with a narrower particle size distribution. Population of relatively large aggregates (2−10 μm) was observed in samples aged from 1 to 3 weeks (Figure 6). The size of the aggregates gradually decreased with the aging time, and after 4 weeks of aging the fraction of 2−10 μm aggregates disappeared. On the other hand, the peak corresponding to the main fraction became broader (Figure 6e), which is probably due to the presence of some small aggregates in the sample. The decrease in the size of aggregates might be due to the homogenization of the system upon prolongation of aging under highly basic media, which leads to more uniform transformation of the aluminosilicate precursors into LTL-type material, thus minimizing abundant aggregation. The aging of the

(45) Barrer, R. M. *Zeolites* **1981**, *1*, 130.
(46) Schriiver, D. F.; Atkins, P. W.; Lanford, C. H. *Inorganic Chemistry*; Oxford University Press: Oxford, 1990; p 27.
(47) Barrer, R. M. *The Hydrothermal Chemistry of Zeolites*; Academic Press: London, 1982; Chapter 4.
(48) Subotic, B.; Graovac, A.; Sekovanic, L. In *Proc. 5th Int. Conf. on Zeolites*; Sersale, R., Colella, C., Aiello, R., Eds.; Giannini: Naples, Italy, 1980; p 54.
(49) Gora, L.; Streletzky, K.; Thompson, R. W.; Phillies, G. D. J. *Zeolites* **1997**, *18*, 119.
(50) Cundy, C. S.; Forrest, J. O.; Plaisted, R. J. *Stud. Surf. Sci. Catal.* **2001**, *135*, 143.

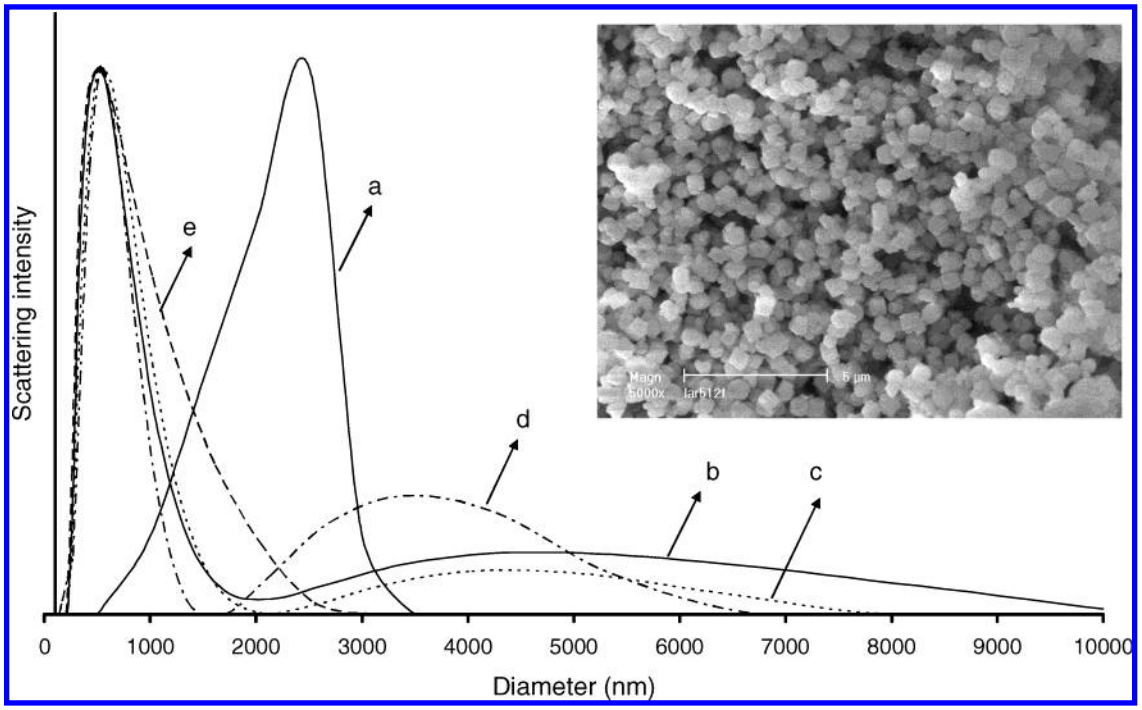

Figure 6. Particle size distribution for the reference sample (a) and products obtained under similar conditions after 1 (b), 2 (c), 3 (d), and 4 weeks (e) aging of the gel at 25 °C. SEM micrograph of the crystal synthesized after 4 weeks aging (inset).

precursor system did not provoke changes in the morphological features of the crystals. The aspect ratio between the prismatic and pinacoidal faces was similar to that of the reference sample (ca. 1) (Figure 6, inset).

Effect of the Temperature. The effect of the crystallization temperature on the morphology of zeolite L was studied in a series of syntheses performed with the reference composition in the temperature range 150−200 °C. No crystalline material was found after 3 days at 150 °C, while a mixture of LTL-type zeolite merlinoite was obtained at 160 °C. The crystals of zeolite L in the latter synthesis were similar to those of the reference sample prepared at 170 °C. The increase of the synthesis temperature to 180 °C resulted in the formation of relatively large (3.0−4.0 μm) crystals. Besides the effect on the crystal size, this synthesis provided crystals with a prismatic/pinacoidal face ratio of about 1.5. This ratio reached 2 in the products obtained at 190 and 200 °C. A relatively high level of aggregation was observed when the higher temperature was used.

Discussion

Aluminosilicate zeolites are synthesized under hydrothermal conditions where the reaction variables include time, temperature, pressure, gel composition, the inorganic and organic cations used, reactant source and type, pH, aging time of the gel, reaction cell fill volume, and so on. The effect of varying one of these parameters is difficult to evaluate in a straightforward manner, because it may have an effect on several others. The reaction system is in general inhomogeneous with both liquid and solid components; thus zeolite nucleation and crystal growth involve numerous simultaneous equilibria and condensation steps, which further complicates the analysis and interpretation of the crystallization process. Hence, to establish a direct relationship between one of these variables and a specific morphological feature is a fairly difficult task.

The results of the present study showed that the factors controlling the nucleation process predetermine the ultimate size of the crystals. For instance, the alkali hydroxide content had a pronounced effect on the crystal size. A 2 times increase of the KOH concentration resulted in the formation of 10 times smaller crystals (Figure 4). Obviously, the increase in the KOH concentration leads to the formation of a larger number of nuclei and thus influences the ultimate crystal size. In other words, the nutrient pool is constant for each system, and the number of viable nuclei formed during the induction period predetermines the ultimate crystal size. Besides the impact on the nucleation process, the concentration of KOH determines strongly the composition of the final product (Figure 4), which shows the interdependence of the factors controlling crystals growth and their effect on the physicochemical properties of the product. A similar effect, that is, a decrease of the size of zeolite L crystals, was achieved by the introduction of limited amounts of barium in the initial gel. This cation strongly influences the nucleation process and, as a consequence, the ultimate size of the crystalline product. The nucleation process can also be influenced by a physical parameter, such as the aging time. Structural rearrangements taking place under ambient conditions provide abundant and uniformly distributed zeolite nuclei, which under hydrothermal treatment provide small uniform zeolite crystals.

The morphology of the crystals, that is, the development of particular crystal faces, is controlled by the dynamic equilibrium during the crystallization process, which is a function of the above-mentioned variables. In the present study, a straight relationship between the water content in the system and the crystal size,

which increases with the dilution of the gel, was found (Figure 1). Besides a gradual increase of the crystal size with the dilution of the gel, remarkable changes of the aspect ratio between the prismatic and pinacoidal faces were observed. It is worth recalling that the differences in the growth rate of different faces determine the crystal morphology. Thus, faces with a high growth rate are less presented or completely absent in the ultimate crystal morphology, while those with a slow growth rate are well developed. Therefore, the observed crystal morphology at low H_2O content suggests a relatively high rate of crystal growth of the prismatic faces ((100) and (1−10)) and a slower growth of the pinacoid (001). In contrast, at high water content, the relatively high growth rate of the pinacoidal face resulted in the formation of long prismatic crystals terminated by small pinacoids (prismatic/pinacoidal = 2−3). A similar effect on the crystal morphology was observed when the crystallization temperature was raised to 180−200 °C. Although a direct relationship between a parameter influences the crystallization process and a specific crystalline morphology is difficult to establish, some information about the growth mechanism can be extracted from the particularities of the zeolite structure and framework composition and the evolution of the system during the crystallization process. For instance, Ohsuna et al.[37] have shown that the framework of LTL-type zeolite is terminated by double 6-rings (D6Rs) on the (001) surface, whereas the four-membered rings (4MRs) of the cancrinite cages are predominantly present on the prismatic walls. On the other hand, Evans and Green[51] have proven that in the LTL-type structure aluminum is preferentially situated in the four-membered rings. Hence, we may speculate that the dilution of the system shifts the equilibrium toward species that are preferentially adsorbed on the pinacoidal face terminated by D6Rs. In such a case, the growth is controlled by low-weight silica-rich species rather than by alumina-rich species. At low water content, the crystal morphology reveals a preferential development of the pinacoidal faces, i.e., the species that are preferentially integrated in the prismatic faces dominate in the mother liquor. The presence of two aluminum atoms in each four-membered ring makes those species aluminum-rich. This speculation is further supported by the observed effect of the KOH content on the crystal morphology. The potassium content in the system $xK_2O{:}0.08Al_2O_3{:}1.0SiO_2{:}15H_2O$ was varied from 0.25 to 0.5, which resulted in crystals with length-to-diameter ratios from 1.0 to 0.5, respectively. The increase of K^+ in the system led to a lower Si/Al ratio in the final product (Figure 4), which correlates well with the preferential development of the pinacoidal faces.

To verify this suggestion, the evolution of the supernatant as a function of the synthesis time for the system $0.25K_2O{:}0.08Al_2O_3{:}1.0SiO_2{:}10H_2O$ was studied. The choice of this system is due to the established preferential growth of one of the crystals faces (Figure 1, see Effect of the Water Content section). The evolution of the composition of the mother liquor was followed by chemical analysis after separating the solid by high-speed centrifugation (Figure 7). There are substantial

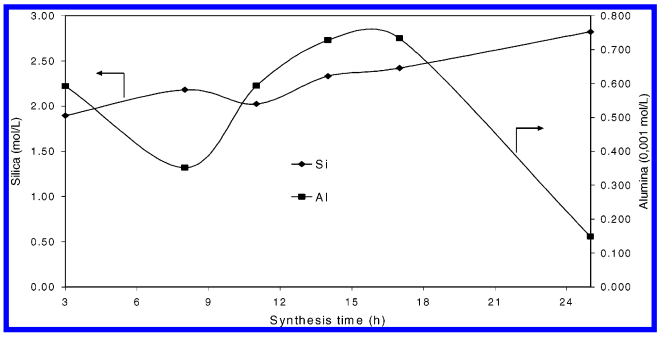

Figure 7. Dissolved silicon and aluminum concentrations of the liquid phase obtained from zeolite L synthesis gels as a function of synthesis time.

fluctuations in the aluminum content in the supernatant. For instance, in the 1−8 h period, the aluminum decreased followed by a sharp increase of the concentration, which continued to 15−16 h crystallization time. This was followed by a relatively sharp decrease of the aluminum content that continued to the end of the crystallization process. The silicon showed completely different behavior, that is, almost a constant increase of its content in the solution was observed. This result is not surprising, having in mind that the Si/Al ratio in the initial gel is 6.25 and about 3 in the crystalline product. The results of the chemical analyses were further coupled with the SEM investigation of the solid. The first crystals were observed after 8 h (Figure 8a) of crystallization, and after 11 h (Figure 8b) the mass of the crystals with respect to amorphous phase was still negligible. The inspection of the crystal morphology showed well-developed pinacoidal faces (1.5−2 μm), with a characteristic overgrowth, and very small prismatic faces (about 200 nm). This period is followed by a substantial increase of the crystal population, but after 17 h of crystallization (Figure 8c) amorphous material is still largely present in the product. Substantial changes in the crystals morphology were not observed during this period. The crystallization process was completed after 25 h (Figure 8d), when only well-shaped coin-like crystals were observed. The characteristic overgrowth on the pinacoidal face still can be seen. However, the prismatic faces were better developed with lengths between 600 and 1000 nm for different crystals in the batch. These data showed that after the onset of the crystallization process and the following stage of mass transformation of the amorphous to crystalline material, the solution is relatively rich in aluminum. During this period, the preferential growth of the prismatic faces led to formation of crystals with large pinacoidal faces and small prismatic ones. Abundant terrace overgrowth of the pinacoidal face is also characteristic for the crystals. The last crystallization stage, when the aluminum content in the mother solution decreased gradually and was almost totally exhausted, is characterized by a preferential growth of the pinacoidal (001) face. This growth resulted in the formation of larger prismatic faces and the disappearance of a part of the terraces overgrown on the pinacoidal one. The growth seems to continue for very long times for some of the crystals, providing tower-like structures on the pinacoidal surface (Figure 8e,f). The diameter of these "towers" decreases from the bottom to the top following the steplike structure of the pinacoidal plane developed

(51) Evans, D. J.; Green, M. *J. Chem. Soc., Chem. Commun.* **1987**, 124.

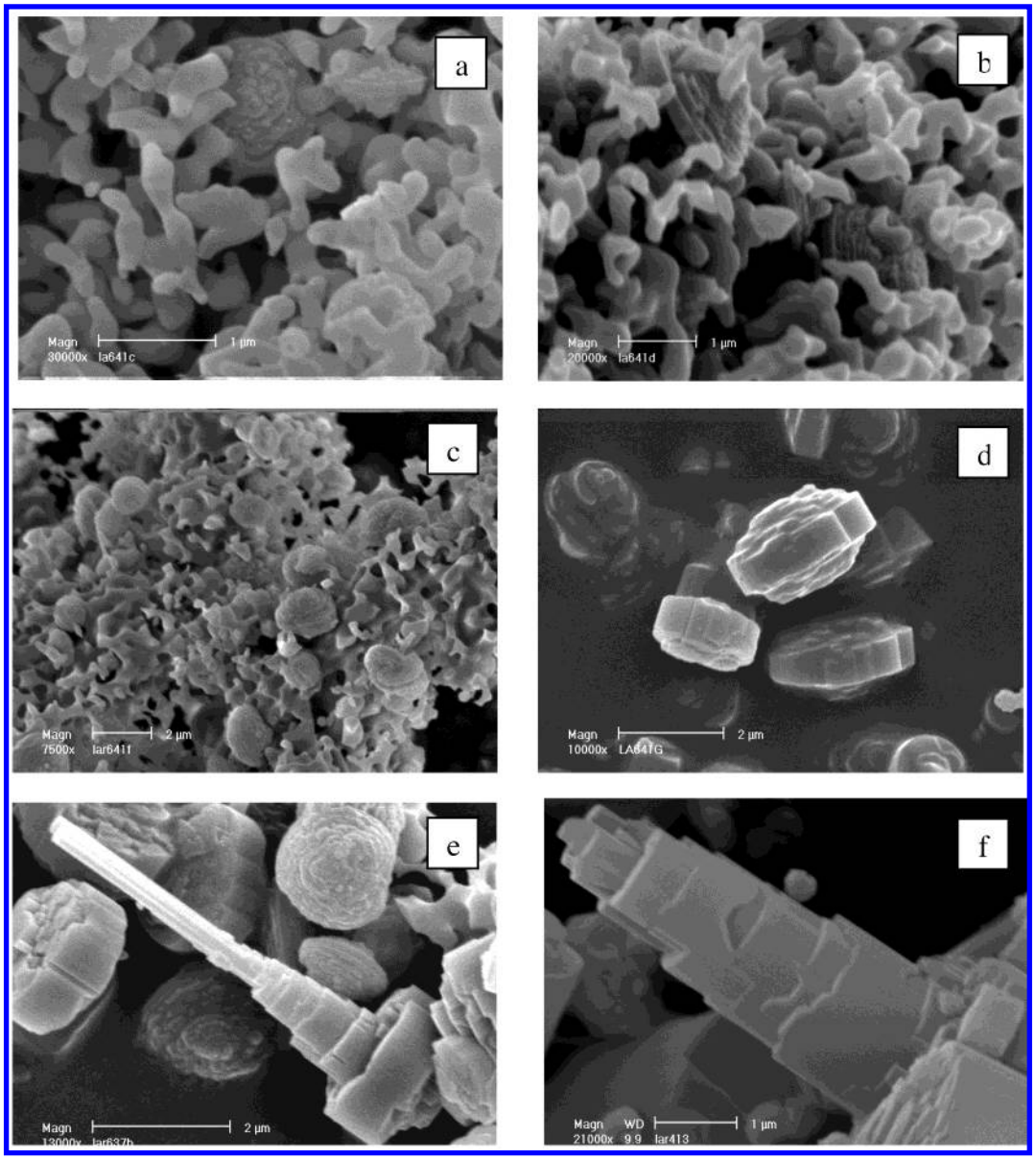

Figure 8. SEM micrographs of the solid obtained after 8 (a), 11 (b), 17 (c), and 25 h (d) of hydrothermal treatment at 170 °C of the system $0.25K_2O:0.08Al_2O_3:1.0SiO_2:10H_2O$. Tower-like structures grown on the pinacoidal face of some of the crystals in the batch (e and f).

during the first stage of crystallization. It is difficult to determine why such an overgrowth is observed on a few crystals only. The factors controlling this growth might be: (i) the presence of active sites on the (001) surface able to ensure the continuous growth in this direction; (ii) local inhomogeneities in the batch; and (iii) limited nutrients at the end of the crystallization process.

The results of this complementary investigation are in good agreement with the suggestion that the preferential growth of the prismatic and pinacoidal faces of zeolite L is controlled by the aluminosilicate species in the mother liquor. Thus, the alumina-rich species lead to preferential growth of the prismatic faces, while the shift of chemical equilibrium to silica-rich precursors promotes the preferential growth of the pinacoidal face.

Conclusions

A detailed study of the chemical and physical parameters that influence the crystal size and morphology of zeolite L was performed. The effect of the water content, concentration of potassium hydroxide, its substitution by sodium hydroxide and small amounts of barium, and the silica/alumina ratio in the initial gel on the crystal habit was investigated. Among the chemical parameters, the water content and the concentration of the potassium hydroxide in the initial gel showed the most pronounced effects. They influenced strongly the crystal habit and the crystal size, respectively. The dilution of the system led to the formation of long prismatic crystals, whereas at low water content crystals with short prismatic faces and coin-like morphology were obtained. The prismatic/pinacoidal faces aspect ratio varied between 0.5 and 3. The increase of the concentration of potassium hydroxide (from $0.25K_2O/SiO_2$ to $0.50K_2O/SiO_2$) resulted in the formation of 1 order of magnitude smaller crystals (from 1 to 2 μm to 150 nm). Substantial reduction of the crystal size was also achieved by introduction of small amounts (from 0.0001

to 0.005 mol of BaO per mol of SiO_2) of barium in the initial gel.

Among the physical parameters, the effects of aging at ambient conditions of the initial gel and of the variation of the crystallization temperature were investigated. A dramatic reduction of the ultimate crystal size, without substantial changes in the prismatic/pinacoidal faces aspect ratio, was obtained after 1 week of aging. Further aging (2−4 weeks) resulted in the crystallization of more uniform in size zeolite particles, but the average crystal size was constant. The increase of the crystallization temperature resulted in the preferential growth of the pinacoidal face, thus providing crystals with higher length-to-diameter ratios.

The investigation provided a detailed picture of the effect and interdependence of different variables influencing zeolite crystallization. The collected data revealed that a preferential growth on the prismatic faces ((100) and (1−10)) takes place when the equilibrium in the system is shifted to alumina-rich species. These faces are terminated by 4MRs where the aluminum is preferentially incorporated. The shift of the equilibrium to silica-rich species results in the growth of the pinacoidal face (001), which is terminated by D6Rs where predominantly the silicon atoms are incorporated.

Generally, the factors controlling the nucleation process predetermine the ultimate crystal size, while those directing the equilibrium during the crystal growth process control the morphology of the crystals. The obtained information can be used for fine-tuning of both the crystal size and the crystal morphology of zeolite L. Thus, the number of pore openings per total external surface of the crystals can be controlled as well as the diffusion paths via the channel system which are expected to have an impact on reaction kinetics.

Acknowledgment. We are grateful to the CNRS/DFG bilateral program for financial support.

Supporting Information Available: X-ray diffraction pattern of zeolite L (PDF). This material is available free of charge via the Internet at http://pubs.acs.org.

CM0498741